

*To appear in: Recent Insights into the Physics of the Sun and Heliosphere
 - Highlights from SOHO and Other Space Missions -
 ASP Conference Series, Vol. 200, 2001
 P. Brekke, B. Fleck, and J. B. Gurman eds.*

The formation of G-band bright points I: Standard LTE modelling

Dan Kiselman

*The Royal Swedish Academy of Sciences, Stockholm Observatory,
 SE-133 36 Saltsjöbaden, Sweden*

Robert J. Rutten

*Sterrekundig Instituut, Postbus 80 000, NL-3508 TA Utrecht, The
 Netherlands*

Bertrand Plez

*GRAAL, Université de Montpellier II, FR-34095 Montpellier Cedex 5,
 France*

Abstract. Assuming LTE, we synthesise solar G band spectra from the semiempirical flux-tube model of Briand & Solanki (1995). The results agree with observed G-band bright-point contrasts within the uncertainty set by the amount of scattered light. We find that it is the weakening of spectral lines within the flux tube that makes the bright-point contrast in the G band exceed the continuum contrast. We also synthesise flux-tube spectra assuming LTE for the full wavelength range from UV to IR, and identify other promising passbands for flux-tube observations.

1. Spectrum synthesis of G-band bright points

Filtergrams taken in the G-band around 430.5 nm are often used for proxy magnetometry since photospheric bright points associated with magnetic structures show up very well in them (e.g. Berger et al. 1995). We have performed LTE spectrum synthesis of the G band (mostly formed by CH) using the semi-empirical magnetic flux-tube model NCHROM7 of Briand & Solanki (1995) which is a refinement of the models of Bruls & Solanki (1993) and Solanki (1986). It is embedded in a standard model for the quiet photosphere.

Figure 1 shows results. The hot bright walls of the (rotationally symmetric) flux tube create a bright ring seen as a double peak in the radiation temperature. Figure 1 also shows the temperature structure along three lines of sight: through quiet sun, through the tube centre, and through the tube wall where the emergent intensity peaks considerably because it samples the quiet-sun model at larger depth than the quiet-sun line of sight does. The peak contrast with respect to the quiet sun is larger in G than in C mainly because the photosphere appears darker in the G band.

Detailed inspection of the synthetic spectra shows how most spectral lines weaken in the flux tube. We interpret this as due to the shallower temperature

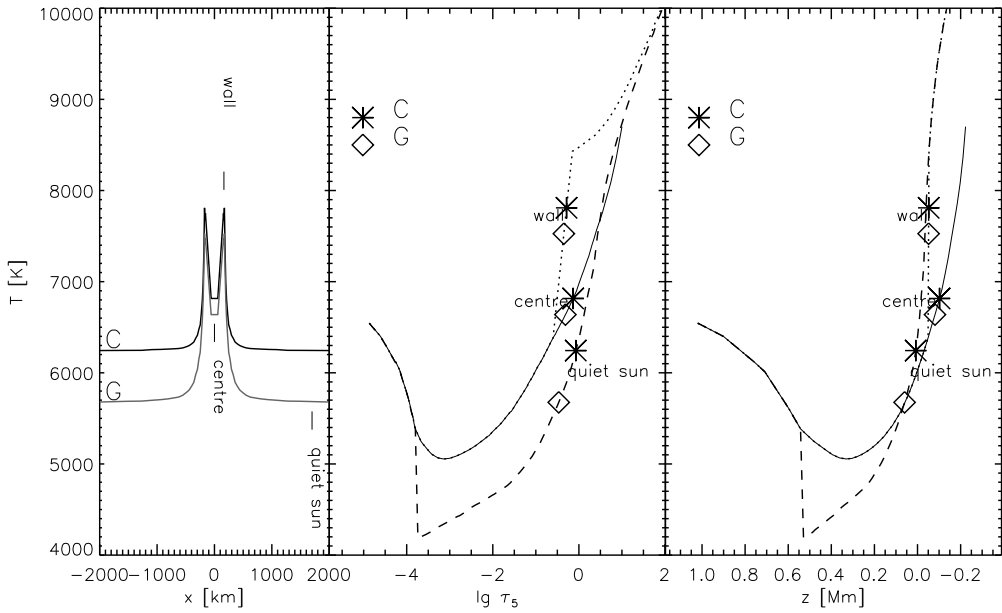


Figure 1. The first panel displays emergent intensity in the form of radiation temperature T_{rad} . The other panels show the kinetic temperature along the three lines of sight indicated in the first panel against optical depth and geometrical height, with the locations where $T_{\text{kin}} = T_{\text{rad}}$ marked. C = continuum, G = G band.

gradient and the lower density inside the flux tube. Molecular lines weaken the most due to the pressure dependence of the molecular association equilibria. This is the reason that bright points should show up particularly well in molecular lines.

2. Comparison with observations

The resulting intensity spectra were integrated using the transmission profiles of two filters that have been used at the Swedish Vacuum Solar Telescope (SVST) on La Palma, denoted G for the G band and C for a nearby continuum band. The results were compared to a pair of G and C images of a solar active region taken with the SVST by Berger & Löfdahl (private communication) and restored by them using the phase-diversity technique (cf. Löfdahl et al. 1998).

Figure 2 compares the contrast values of the two passbands – i.e. the spectrally integrated intensity (G and C) normalised to the quiet sun intensity ($\langle G \rangle$ and $\langle C \rangle$) – with the observations. The points and contours represent the G and C contrasts measured per pixel in the SVST images. The stars represent peak intensities from the flux tube model after convolution with a range of smearing functions that simulate degradation by atmospheric seeing and by the telescope. The resulting peak contrast is very sensitive to the far wings of the smearing profile – which are very difficult to assess. Nevertheless, the comparison indicates

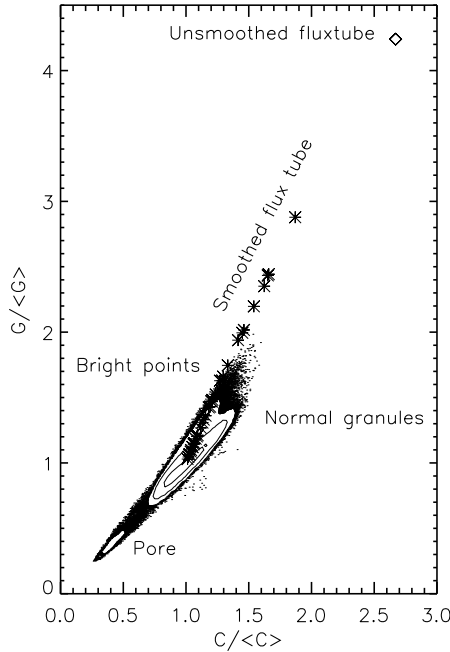


Figure 2. Observed normalised intensities (points and contours) and synthesised flux-tube peak intensities for different smoothing values (stars and diamond).

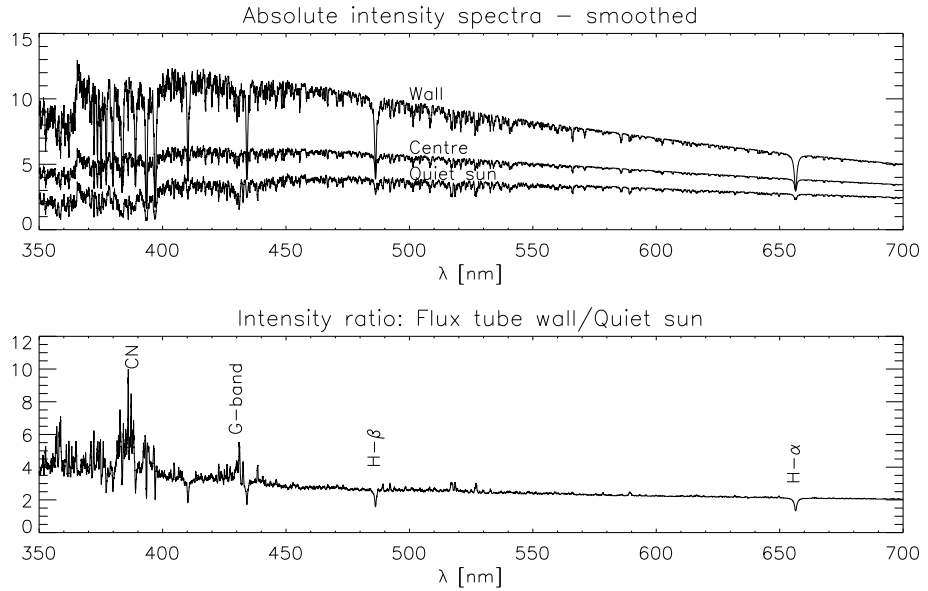


Figure 3. Upper panel: entire optical spectrum from the three lines of sight indicated in Fig. 1. Lower panel: maximum contrast with the outside quiet photosphere.

reasonable agreement between the computed peak contrasts and the highest observed contrasts.

3. Flux-tube signatures in other spectral bands

Could there be other spectral regions useful for proxy magnetometry or flux-tube diagnostics? We synthesised also a wide range of the solar spectrum with spectral resolution $R = 20000$. The upper panel of Fig. 3 shows smoothed spectra along the three lines of sight indicated at left in Fig. 1. The lower panel shows the wall/quiet-sun contrast. The Balmer lines stand out because they get stronger due to the high temperature of the flux-tube walls. The Balmer jump does not strengthen, however, so that feature is probably not a good flux-tube diagnostic.

The violet CN band produces large contrast in the lower panel of Fig. 3 and is known to display the photospheric network well (Chapman 1970). Inspection of the computed molecular equilibria shows that CN is depleted to a smaller fraction in the flux tube than CH. Preliminary results from the SVST received during the symposium (Rouppe van der Voort, private communication) confirm indeed that CN bright points look very similar to those seen in the G band.

4. Conclusions

The Briand & Solanki model produces bright-point contrasts similar to those observed at the SVST. However, the spectrum synthesis was made assuming LTE and the photospheric part of the flux tube model was primarily constructed from LTE inversions of spectropolarimetric data. Do we believe these LTE assumptions? Not necessarily. A contrasting scenario would be one where UV radiation from the hot walls photodissociates CH in the flux tube and also causes overionisation of metals, thus affecting our G-band synthesis as well as the semi-empirical modelling. If there is any place in the solar photosphere where 3D–NLTE effects are important, it should be in these flux tubes.

Acknowledgments. Carine Briand and Sami Solanki very kindly provided their flux-tube models and software to handle them plus instructions. Mats Löfdahl and Tom Berger generously shared their observational data.

References

Berger, T.E., Schrijver, C.J., Shine, R.A., Tarbell, T.D., Title, A.M., Scharmer, G.B. 1995, ApJ, 454, 531
 Chapman, G.A. 1970, Sol. Phys., 13, 78
 Briand, C., Solanki, S.K. 1995, A&A, 299, 596
 Bruls, J.H.M.J., Solanki, S.K. 1993, A&A, 273, 293
 Löfdahl, M.G., Berger, T.E., Shine, R.S., Title, A.M. 1998, ApJ, 495, 965
 Rutten, R.J. 1999, ASP Conf. Series 184, 181
 Solanki, S.K. 1986, A&A, 168, 311